Search and rescue: tackling antibiotic resistance with chemistry

Wade, N.

Citation

Wade, N. (2024, January 17). *Search and rescue: tackling antibiotic resistance with chemistry*. Retrieved from https://hdl.handle.net/1887/3713759

Note: To cite this publication please use the final published version (if applicable).

Chapter 5

Implementation of an LspA FRET assay to aid the development of peptidomimetic inhibitors

1. Introduction

The steady development of new resistance mechanisms able to evade treatment with most clinically used antibiotics has led to multi-drug resistant (MDR) pathogens, which are a major concern to public health.[1–3] As a result, the development of new antibiotics is vital in the attempt to tackle these dangerous pathogens. Identifying and exploiting essential pathways which have not been the subject of targeted discovery is therefore of paramount importance. Research lines that follow this approach hold promise to find novel antibiotics able to tackle MDR pathogens.

A promising target for antibiotic development is lipoprotein signal peptidase II (LspA), a crucial bacterial enzyme involved in the maturation of lipoproteins. Located at the inner-membrane, LspA cleaves a membrane-anchoring signal peptide from pre-lipoproteins to give the lipoprotein.[4] The product can be further processed through acylation of the free amine released by this cleavage before ultimately being transported to the outer membrane.[5] Inhibition of LspA causes a build-up of pre-lipoproteins in the cell,[6] as was noted when natural product LspA inhibitors globomycin and myxovirescin were discovered.[7–9] This pre-lipoprotein accumulation has been shown as being lethal to bacterial cells, making LspA an attractive target for inhibitor development.[10,11]

For the rational design of inhibitors, one must consider the active site of the target enzyme. LspA is an aspartyl protease, a class of enzymes which utilises two aspartic acid residues to cleave a robust amide bond.[12] In the case of LspA, the peptide bond cleavage results in the separation of the signal peptide from the lipoprotein, which is a key step in lipoprotein maturation. The aspartic acid side chains activate a water molecule, which subsequently performs a nucleophilic attack on the carbonyl of the target amide, forming a tetrahedral intermediate.[13] This intermediate then rearranges, resulting in a terminal carboxylic acid on the signal peptide and a primary amine on the lipoprotein (**Figure 1**).

Designing inhibitors for aspartyl protease enzymes of clinical relevance has previously proved successful, with many compounds being tested in clinical trials and some approved for clinical use.[14,15] Many inhibitors of this enzyme class are transition-state mimics, which contain non-cleavable motifs resembling the intermediate tetrahedral structure produced during the amide-cleaving step.
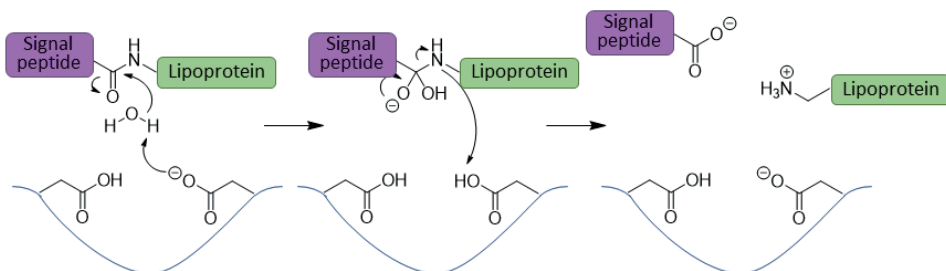
Figure 1. The proposed mechanism of peptide bond cleavage between the signal peptide and lipoprotein by LspA. A water molecule is activated by an aspartic acid residue for nucleophilic attack on the targeted carbonyl. The tetrahedral intermediate then rearranges and the amine group leaves to separate the lipoprotein from the signal peptide.

At the forefront of aspartyl protease inhibitor design is the large body of work concerning HIV-1 protease, an essential enzyme required for the production of mature and virulent HIV virions.[14] Many generations of peptidomimetics have been made in the attempt to develop inhibitors of HIV-1 protease as treatment for HIV/AIDS, each one with improved potency towards the protease as well as with better physicochemical properties. In the case of HIV-1, most first-generation inhibitors contained either a hydroxyethylene or hydroxyethylamine transition-state mimic within their structure (**Figure 2A**). Another well-studied aspartyl protease is the enzyme renin, which is involved in the angiotensin pathway in the human body and regulates blood pressure. Inhibitors of this enzyme can therefore be used to treat hypertension. The statin and hydroxyethylene transition-state mimics were found to be effective in peptidomimetics for renin (**Figure 2B**).[16–18] There are many other transition state mimics which have been used in peptidomimetic inhibitors of aspartyl protease enzymes, and some examples of these structures are shown in **Figure 2C**.

Despite the large number of antibiotics that have been approved for clinical use, there are no antibiotics that belong to the aspartyl protease inhibitor class. With the identification of LspA as an essential aspartyl protease needed for bacterial growth, the development of an inhibitor for this enzyme could lead to novel antimicrobial drugs. With this in mind, we wanted to use the well-documented peptidomimetic development route to generate inhibitors of LspA. In doing so, I collaborated with Martin group colleague Ned Buijs who designed and synthesized

a number of novel peptidomimetics that I in turn tested as inhibitors of LspA using the assay described in the preceding chapter. The starting point for these peptidomimetic LspA inhibitors was a truncated structure resembling the natural substrate of the enzyme. From there, a number of analogues were prepared containing one of the non-cleavable motifs described above at the cleavage site. The peptidomimetic scaffold employed is based on the natural substrate for LspA, specifically the amino acids on either side of the amide bond cleaved by LspA (**Figure 3A**). The N-terminus was capped with an acetyl group and the C-terminus was prepared as the primary amide by the use of Rink amide resin during solid-phase peptide synthesis (SPPS). The non-cleavable motifs chosen were the reduced amide, difluoroalcohol, hydroxymethylcarbonyl (HMC), and statin (**Figure 3B**). In addition, the diacylglycerol lipid from the FRET substrate was replaced with simpler lipids, a benzyl or octyl chain. The resulting library of peptidomimetics is summarized in **Figure 3B.** All compounds were next assessed by means of the FRET assay described in Chapter 4 to quantify their ability to inhibit LspA.
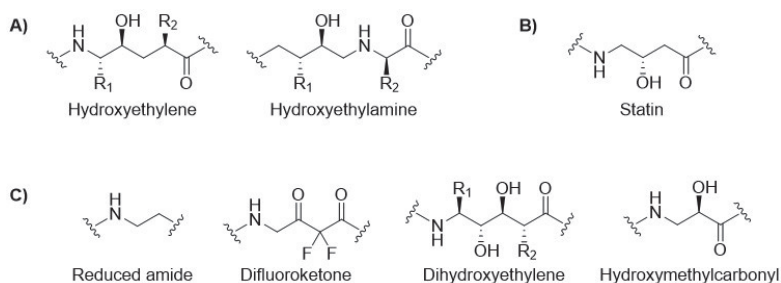

Figure 2. A) Structures of the non-cleavable motifs hydroxyethylene and hydroxyethylamine used in first-generation HIV-1 inhibitors. B) Structure of the statin non-cleavable motif used in inhibitors of renin. C) Structures of other non-cleavable motifs used in aspartyl protease inhibitors.

2. Results and discussion

2.1 LspA Assay

The LspA assay used for evaluating the peptidomimetic inhibitors employed the FRET substrate provided by the Caffrey group (**Figure 4A**). A Michaelis-Menten experiment was first conducted with LspA at 50 nM to establish the K_m and V_{max} values of the enzyme-substrate pair, which were 17.0 μM and 7.0 μM/sec respectively (**Figure 4B**). The K_m value thus

determined was used as the substrate concentration for the subsequent inhibitor testing experiments.
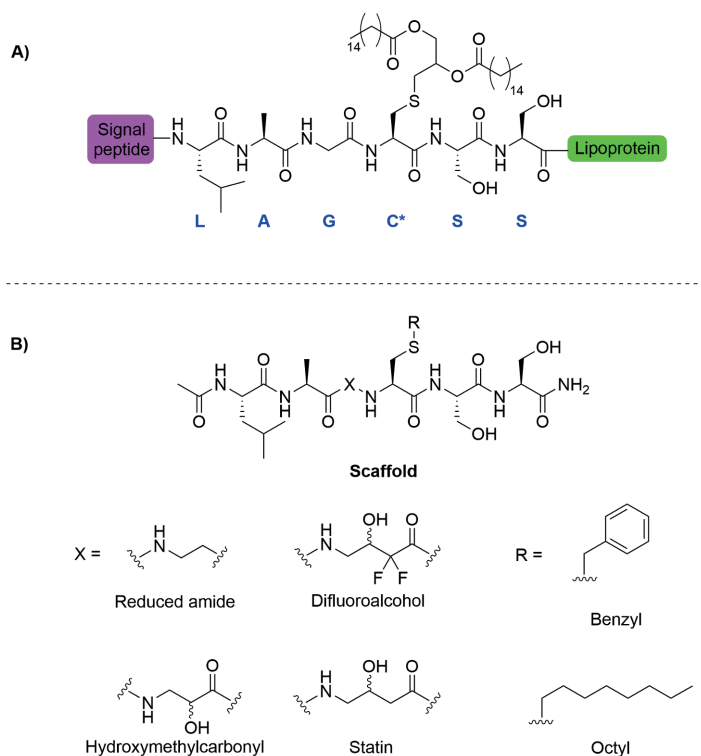

Figure 3. A) Structure of the LspA substrate containing the amino acid sequence the scaffold is based on. Single letter amino acid code is written in blue. * represents the diacylglycerol group on cysteine. B) Structure of the peptidomimetic scaffold. X represents the non-cleavable motif that replaces the glycine residue in the natural substrate. R represents the lipid replacing the diacylglycerol of the natural substrate.

2.2 Testing of first generation peptidomimetics

With suitable enzyme/substrate concentrations determined, the peptidomimetic compounds were next evaluated for LspA inhibition. The structures of each compound are shown in **Figure 5**, with the non-cleavable motif used (either reduced amide, difluoroalcohol, HMC or statin) highlighted by a blue box. Different lipophilic moieties were also tested: octyl and benzyl chains were incorporated with each of the non-cleavable motifs. All compounds were synthesised as mixture of diastereomers, some of which were separable during the purification

process. When applicable, the diastereomeric peptidomimetics were tested individually and were labelled **a** or **b** depending on the HPLC elution order (**a** for first peak, **b** for second peak).
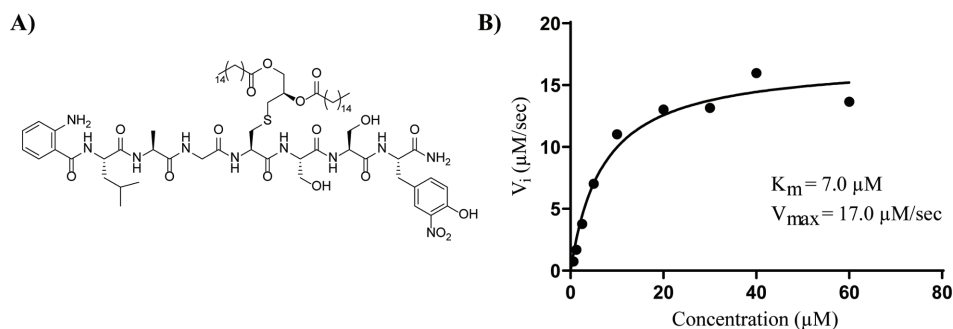
A)

B)

$K_m = 7.0\ \mu M$
$V_{max} = 17.0\ \mu M/sec$

Figure 4. A) Structure of FRET substrate used in the assay, provided by Martin Caffrey and colleagues. B) The Michaelis-Menten plots for LspA with substrate provided by Martin Caffrey and colleagues. Several concentrations of substrate were mixed with LspA (50 nM), and the initial velocity of each slope was measured. The substrate concentration and corresponding initial velocity values were plotted on Graphpad Prism. The values of V_{max} and K_m were 17.0 μM and 7.0 $\mu M/sec$ respectively.

Each compound was first assessed for inhibition activity at a single concentration (500 μM). LspA (50 nM) and substrate (7 μM) were added, and the fluorescence output was measured (Ex: 320 nm, Em: 420 nm) over 1 hour. As a comparison, the natural product LspA inhibitor, globomycin, was taken as a positive control to observe the signal when the enzyme is fully inhibited.[19] As a negative control, the enzyme and substrate were combined with no additional compound to observe the maximum gradient of the FRET signal. Percentage inhibition of the enzyme was then calculated in reference to the positive and negative controls of each experiment. Out of the compounds tested, the peptidomimetics containing a hydroxymethylcarbonyl motif **5a** and **5b** were found to be the most active inhibitors, with inhibition values of above 80%. The fluorescence value measured at the zero time-point for compound **5a** was higher than that of globomycin which may be caused by the compound itself giving a fluorescent readout at 420 nm. However, by the end of the experiment the fluorescence readout was roughly the same value. This phenomenon, combined with a natural loss of volume in the reaction wells arising from the long reaction time at an elevated temperature, resulted in a steeper decrease in gradient compared to the globomycin control and an inhibition percentage of 118%. The complete lack of activity of compound **6** was surprising, considering that the

same non-cleavable motif in compounds **5a** and **5b** was used and the only difference being a benzyl side chain instead of octyl. The compounds containing the reduced amide and difluoroketone non-cleavable motifs (**1-4**, **Figure 5**) were found to only weakly inhibit LspA, with compound **3** and **4a** reaching 65% and 68% inhibition respectively. Peptidomimetics containing the statin moiety also has little effect on the activity of LspA, with inhibition values lower than 20% for both the octyl (**7**) and benzyl (**8**) compounds.
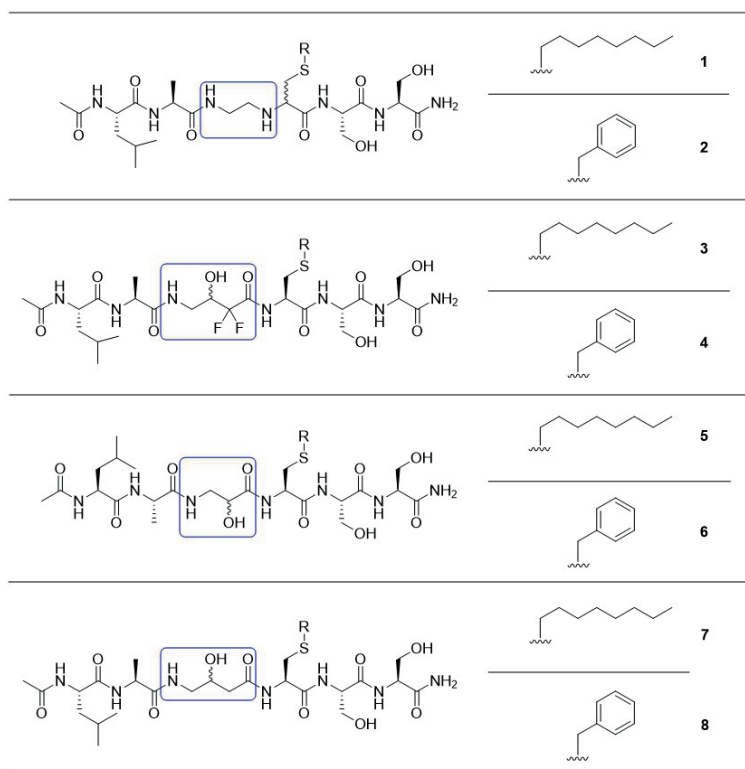

Figure 5: Structures of the peptidomimetics designed to test different non-cleavable motifs and lipophilic fragments. Non-cleavable motifs: reduced amide **1a/b** & **2a/b**; difluoroalcohol **3** & **4a/b**; hydroxymethylcarbonyl **5a/b** & **6**; statin **7** & **8**.

The top performing compound from each diastereomer pair was chosen for further analysis as the previous experiment gave only a snapshot of the inhibition profile at a single concentration of inhibitor. No further testing was carried out on the compounds containing the statin non-cleavable motif due to lack of activity at 500 μM. The determination of IC_{50} values for peptidomimetics **1-3** was restricted due to DMSO concentration restrains, which resulted in the

highest concentration of compound tested not being able to fully inhibit the enzyme. In these cases, an exact IC_{50} value could not be calculated but it can be stated that the value would be >300 µM. When the assay was run with compounds **4a** and **5a**, instead, complete inhibition curves could be obtained and the IC_{50} values were found to be 234 µM and 181 µM respectively.

Table 1. IC_{50} values of the top performing compounds from each diastereomer pair.

IC_{50} (µM)

4a: 234

5a: 181

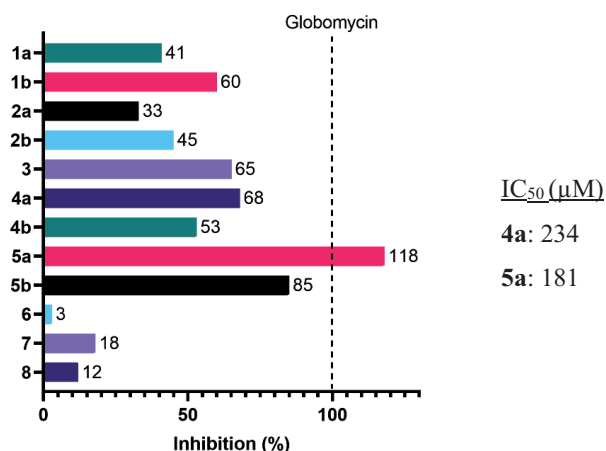**Figure 6**. Chart showing percentage inhibition of LspA at 500 µM of inhibitor. Measurements were taken over a 1-hour period and the increase in fluorescent gradient was normalized to the positive and negative control to give a percentage inhibition. Globomycin line indicates fully inhibited enzyme. The IC_{50} values of compound **4a** and **5a** are also indicated.

3. Conclusion

A panel of peptidomimetics was assessed for inhibition of the bacterial aspartyl protease, LspA, using the FRET assay described in Chapter 4. The peptidomimetics were designed to mimic the natural substrate of LspA and were initially tested at a single concentration (500 µM) to assess for inhibition of LspA. These studies indicated that peptidomimetic **5a**, containing a hydroxymethylcarbonyl (HMC) non-cleavable motif paired with the octyl chain, is the most active LspA inhibitor of the series, fully inhibiting the enzyme at 500 µM. The diastereomer from each compound pair with the highest percentage inhibition was subjected to a full IC_{50} experiment. An accurate value for most compounds could not be established as the concentration of inhibitor required to fully inhibit the enzyme was not achievable due to

solubility limitations. However, complete inhibition curves were obtained for compounds **4a** and **5a**, which were found to exhibit IC$_{50}$ values of 234 μM and 181 μM respectively. With this in mind, the peptidomimetic **5a** featuring the HMC non-cleavable motif together with the octyl side chain appears to be the best candidate for further modification in the pursue of compounds with lower IC$_{50}$ values and better physicochemical properties.
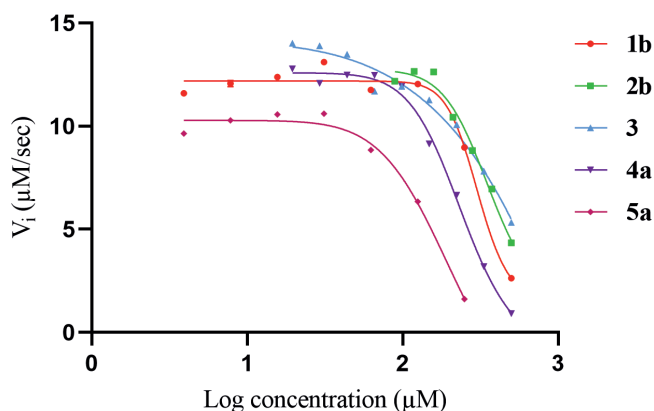

Figure 7. IC$_{50}$ curves of the top performing compounds against LspA (50 nM).

4. Materials and Methods

4.1 Enzyme experiments

Expression and Purification. The plasmid LspA-pET28a was received from the Caffrey group, transformed into *E. coli* BL21(DE3) and plated on kanamycin plates. Three colonies were used to inoculate 3 x 50 mL LB supplemented with kanamycin and incubated overnight at 37 °C with shaking. The overnight cultures (20 mL/flask) were then used to inoculate 6 x 1 L of Lysogeny Broth (LB) supplemented with kanamycin (50 mg/L) and incubated at 37 °C for 2.5 h. Once the culture reached an OD600 of 0.75, LspA expression was induced by the addition of IPTG (final concentration: 1 mM) which was then incubated overnight at 30 °C. The cells were harvested by centrifugation (5000xg) at 24 °C and stored at -80 °C for two weeks. The cell pellet was resuspended in 80 mL of buffer 1 (50 mM MES pH 6.5, 150 mM NaCl, 10% (v/v) glycerol) and then lysed by sonication. The lysed cells were then centrifuged (12000xg) for 30 minutes before the supernatant was removed and centrifuged again (55000xg) for 60 minutes. The membrane pellet was resuspended using a dounce homogenizer in 12 mL of

buffer 1. The enzyme was aliquoted (1 mL) and stored at -80 °C. Three aliquots were combined and diluted to 16 mL with buffer 1 then supplemented with the detergent FC-12 to a final concentration of 1% (w/v). The membranes were then centrifuged (100000xg) for 60 minutes to remove the insoluble material. The supernatant was collected and supplemented with imidazole (20 mM) before being added to nickel resin (prewashed with buffer 2 (50 mM MES pH 6.15, 150 mM NaCl, 10% (v/v) glycerol, 0.14 % (w/v) FC-12)). This suspension was mixed at 4 °C for 60 minutes. The suspension was added to a gravity column and washed with buffer 3 (50 mL, 50 mM MES pH 6.15, 150 mM NaCl, 10% (v/v) glycerol, 0.14% FC-12, 50 mM imidazole). LspA was then eluted from the resin with buffer 4 (50 mM MES pH 6.15, 150 mM NaCl, 10% (v/v) glycerol, 0.14% FC-12, 50 mM imidazole) and collected in 1 mL fractions until it was no longer detectable by nanodrop. The eluted fractions were combined, concentrated and washed with buffer 1 until the imidazole concentration is below 1%.

Percentage inhibition assay. Test compounds were diluted in buffer to 2x final concentration. LspA and FRET substrate were diluted in buffer to 4x their final concentration. Globomycin (500 nM final concentration) was used as a positive control and the negative control wells had no additional compound. The compounds were incubated at 37 °C with LspA (12.5 µL, 50 nM final concentration) for 10 minutes with shaking every 30 s. LspA FRET substrate was then added to the plate (12.5 µL, 7 µM final concentration, 50 µL final volume), before measuring the fluorescence readout at 30 s intervals for 50 minutes at 37 °C. Using the initial velocity data of the compounds and the controls, the percentage of LspA inhibited by 500 µM of each compound was calculated. The buffer used was 100 mM MES/NaOH pH 5.4, 150 mM NaCl, 0.05% (w/v) LMNG and the final concentration of DMSO in the experiment was 10%. Fluorescence readout was measured on a Tecan Spark plate reader (Ex: 320 nm, Em: 420 nm). Microplates used were µClear®, black half-area 96-well plate (Greiner Bio-one).

IC_{50} *assay.* The half-maximal inhibitory concentration (IC_{50}) of each compound was determined against LspA. The compounds were diluted to 2x final concentration and serially diluted (25 µL). The compounds were incubated with LspA (12.5 µL, 50 nM final concentration) for 10 minutes at 37 °C, shaking every 30 s. LspA FRET substrate (12.5 µL, 7 µM final concentration, 50 µL final volume) was added and fluorescence was measured at 30 s intervals for 50 minutes at 37 °C. The initial velocity data was used to produce IC_{50} curves in GraphPad Prism 7 software. The buffer used was 100 mM MES/NaOH pH 5.4, 150 mM NaCl, 0.05% (w/v) LMNG and the final concentration of DMSO in the experiment was 10%.

Fluorescence readout was measured on a Tecan Spark plate reader (Ex: 320 nm, Em: 420 nm). Microplates used were μClear®, black half-area 96-well plate (Greiner Bio-one).

5. References

1   M. Frieri, K. Kumar and A. Boutin, *J. Infect. Public Health*, 2017, **10**, 369–378.

2   H. Nikaido, *Annu. Rev. Biochem.*, 2009, **78**, 119–146.

3   G. Mancuso, A. Midiri, E. Gerace and C. Biondo, *Pathogens*, 2021, **10**, 1–14.

4   N. Buddelmeijer, *FEMS Microbiol. Rev.*, 2015, **39**, 246–261.

5   M. M. Wilson and H. D. Bernstein, *Trends Microbiol.*, 2016, **24**, 198–208.

6   M. Hussain, S. Ichihara and S. Mizushima, *J. Biol. Chem.*, 1980, **255**, 3707–3712.

7   M. Inukai, R. Enokita, A. Torikata, M. Nakahara, S. Iwado and M. Arai, *J. Antibiot.,* 1978, **31**, 410–420.

8   M. Inukai, M. Nakajima, M. Ōsawa, T. Haneishi and M. Arai, *J. Antibiot.,* 1978, **31**, 421–425.

9   Y. Xiao, K. Gerth, R. Müller and D. Wall, *Antimicrob. Agents Chemother.*, 2012, **56**, 2014–2021.

10   D. G. Brown, T. Lister and T. L. May-Dracka, *Bioorganic Med. Chem. Lett.*, 2014, **24**, 413–418.

11   S. Kitamura, A. Owensby, D. Wall and D. W. Wolan, *Cell Chem. Biol.*, 2018, **25**, 301–308.

12   D. R. Davies, *Annu. Rev. Biophys. Biophys. Chem.*, 1990, **19**, 189–215.

13   B. Veerapandian, J. B. Cooper, A. Šali, T. L. Blundell, R. L. Rosati, B. W. Dominy, D. B. Damon and D. J. Hoover, *Protein Sci.*, 1992, **1**, 322–328.

14   A. K. Ghosh, H. L. Osswald and G. Prato, *J. Med. Chem.*, 2016, **59**, 5172–5208.

15   Y. Hamada and Y. Kiso, *Biopolymers*, 2016, **106**, 563–579.

16   F. Gross, J. Lazar and H. Orth, *Science*, 1972, **175**, 656.

17   D. H. Rich, *J. Med. Chem.*, 1985, **28**, 263–273.

18   R. Göschke, N. C. Cohen, J. M. Wood and J. Maibaum, *Bioorganic Med. Chem. Lett.*, 1997, **7**, 2735–2740.

19   I. K. Dev, R. J. Harvey and P. H. Ray, *J. Biol. Chem.*, 1985, **260**, 5891–5894.